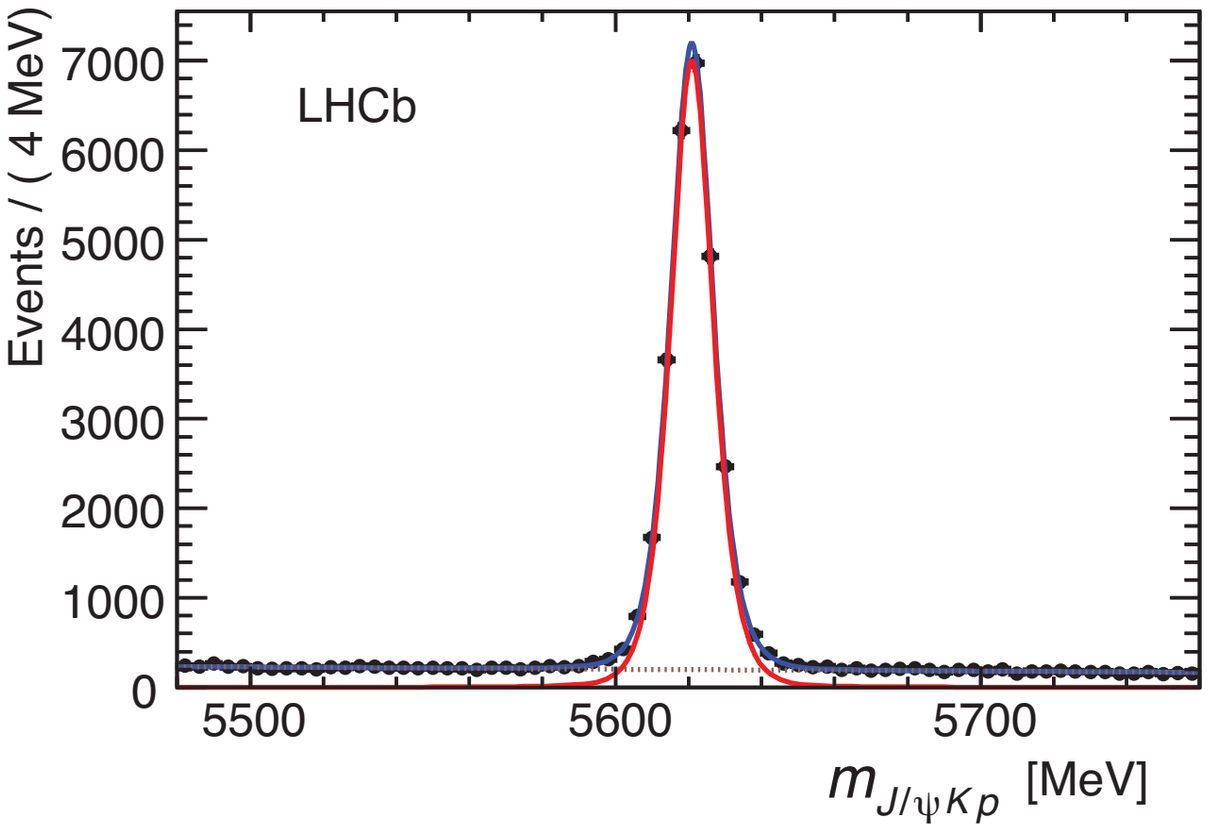

Figure 4: Invariant mass spectrum of $J/\psi K^- p$ combinations, with the total fit, signal and background components shown as solid (blue), solid (red) and dashed lines, respectively.

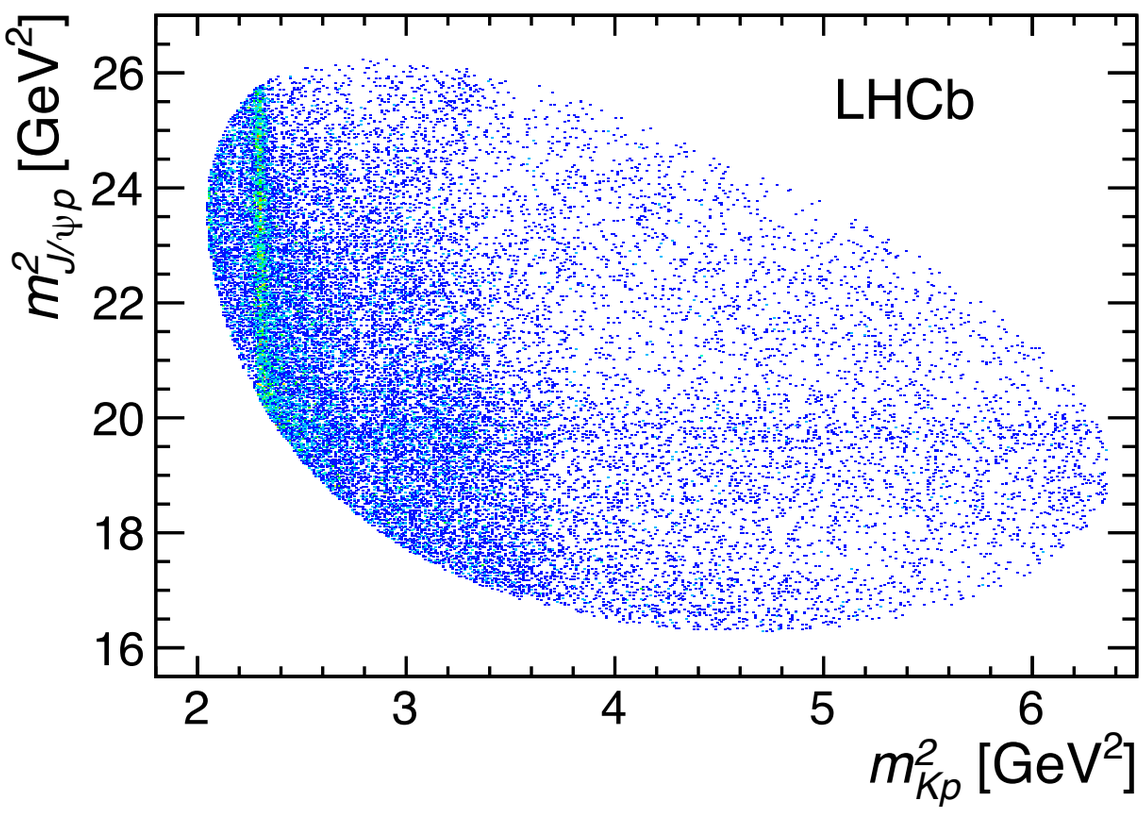

Figure 5: Invariant mass squared of $K^- p$ versus $J/\psi p$ for candidates within ± 15 MeV of the Λ_b^0 mass.

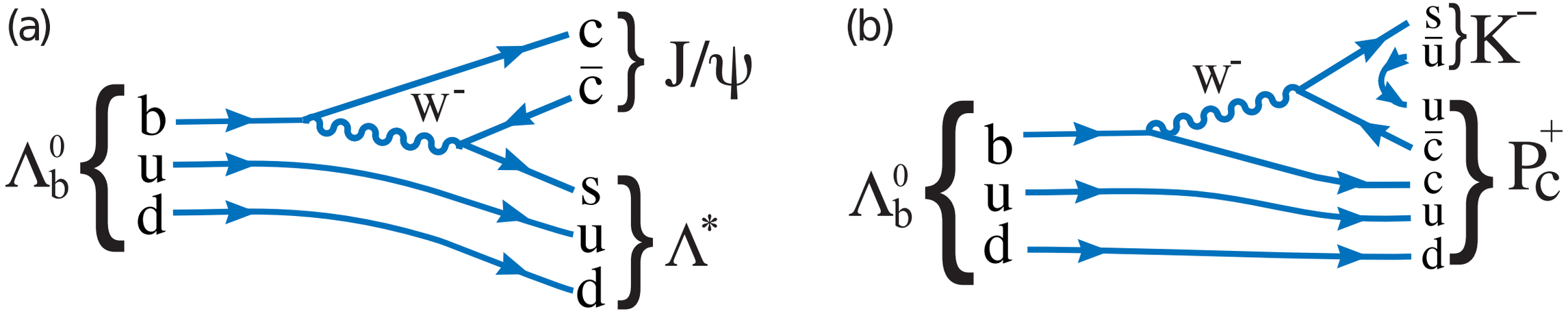

Figure 1: Feynman diagrams for (a) $\Lambda_b^0 \to J/\psi\, \Lambda^*$ and (b) $\Lambda_b^0 \to P_c^+ K^-$ decay.

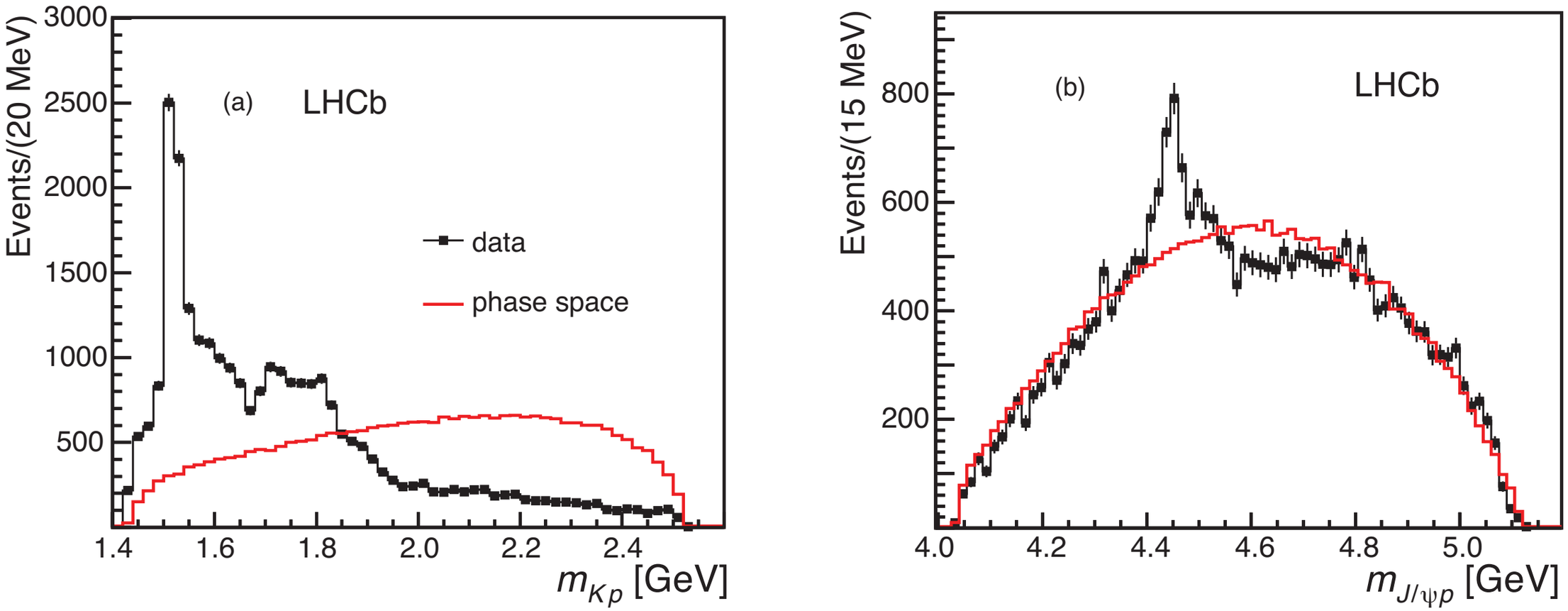

Figure 2: Invariant mass of (a) K^-p and (b) $J/\psi\, p$ combinations from $\Lambda_b^0 \to J/\psi\, K^-p$ decays. The solid (red) curve is the expectation from phase space. The background has been subtracted.

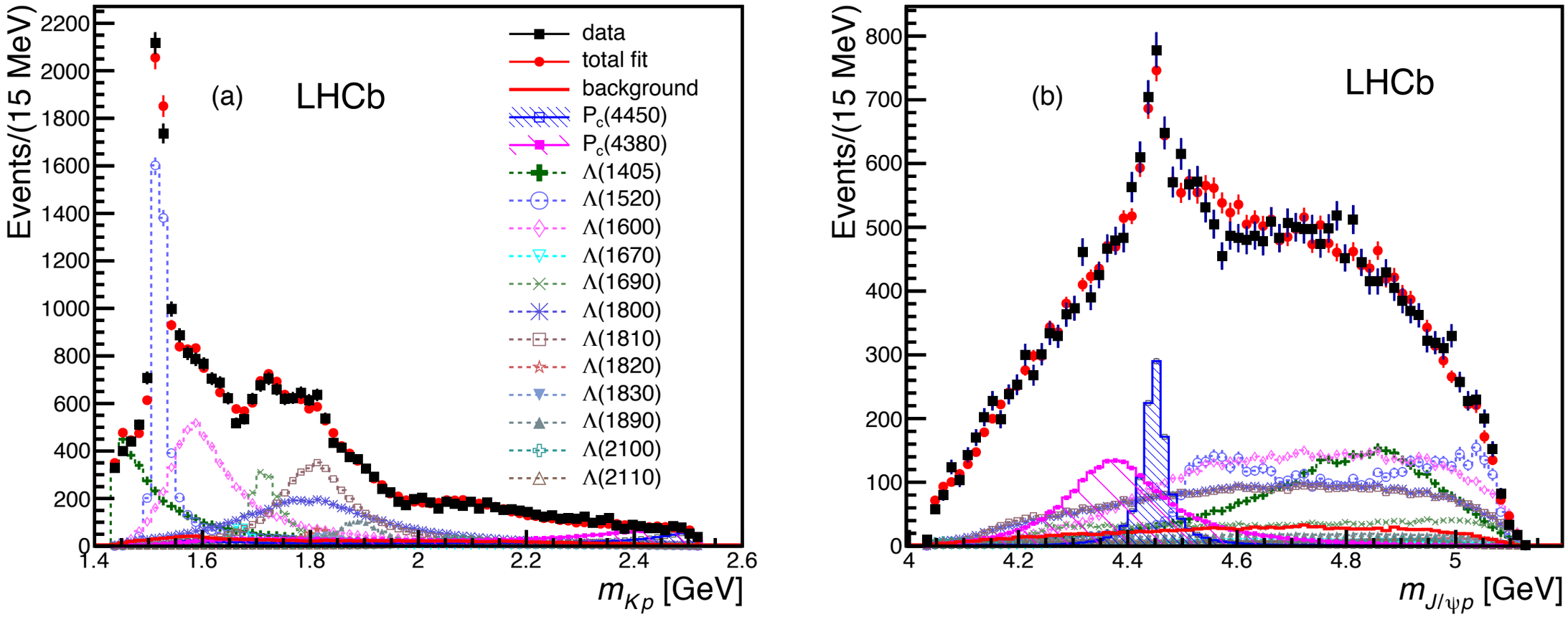

Figure 3: Fit projections for (a) m_{Kp} and (b) $m_{J/\psi p}$ for the reduced Λ^* model with two P_c^+ states (see Table 1). The data are shown as solid (black) squares, while the solid (red) points show the results of the fit. The solid (red) histogram shows the background distribution. The (blue) open squares with the shaded histogram represent the $P_c(4450)^+$ state, and the shaded histogram topped with (purple) filled squares represents the $P_c(4380)^+$ state. Each Λ^* component is also shown. The error bars on the points showing the fit results are due to simulation statistics.

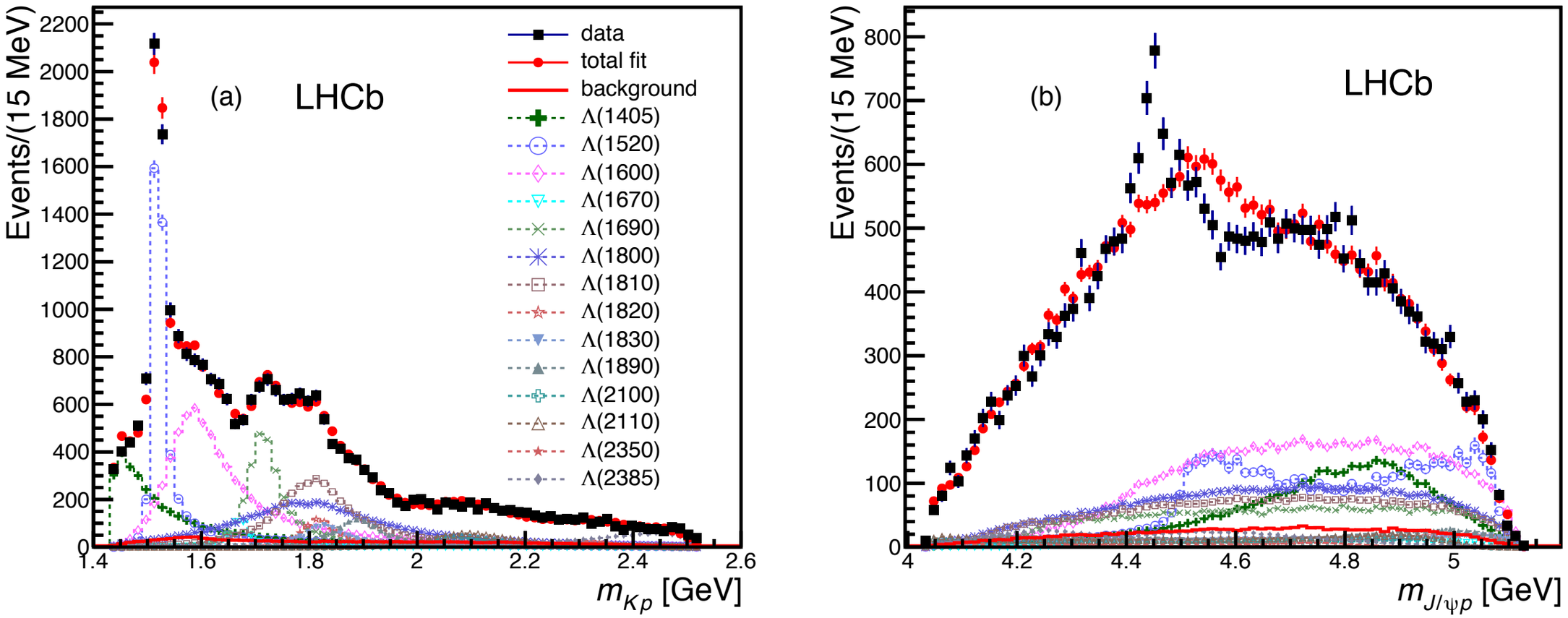

Figure 6: Results for (a) m_{Kp} and (b) $m_{J/\psi p}$ for the extended Λ^* model fit without P_c^+ states. The data are shown as (black) squares with error bars, while the (red) circles show the results of the fit. The error bars on the points showing the fit results are due to simulation statistics.

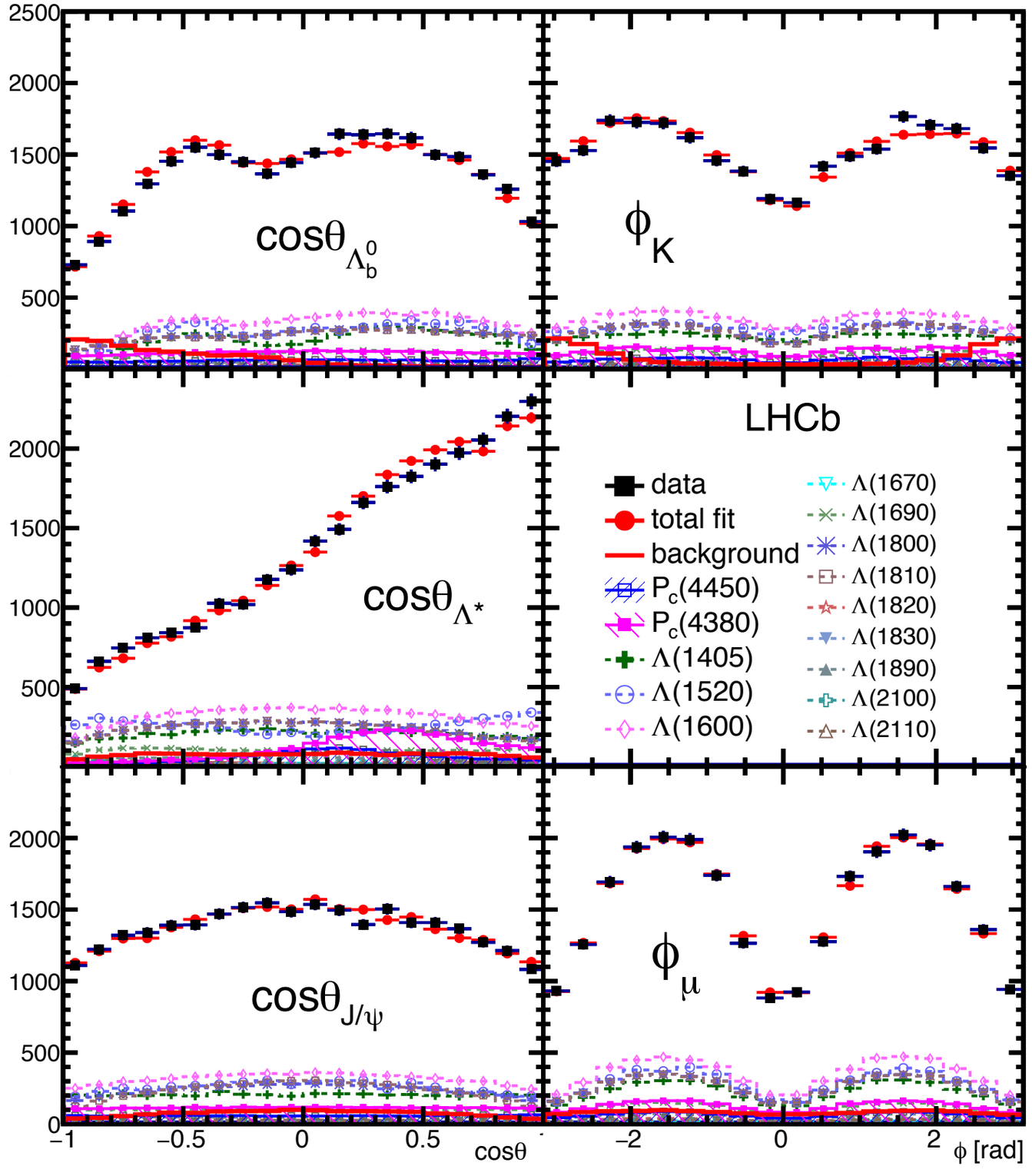

Figure 7: Various decay angular distributions for the fit with two P_c^+ states. The data are shown as (black) squares, while the (red) circles show the results of the fit. Each fit component is also shown. The angles are defined in the text.

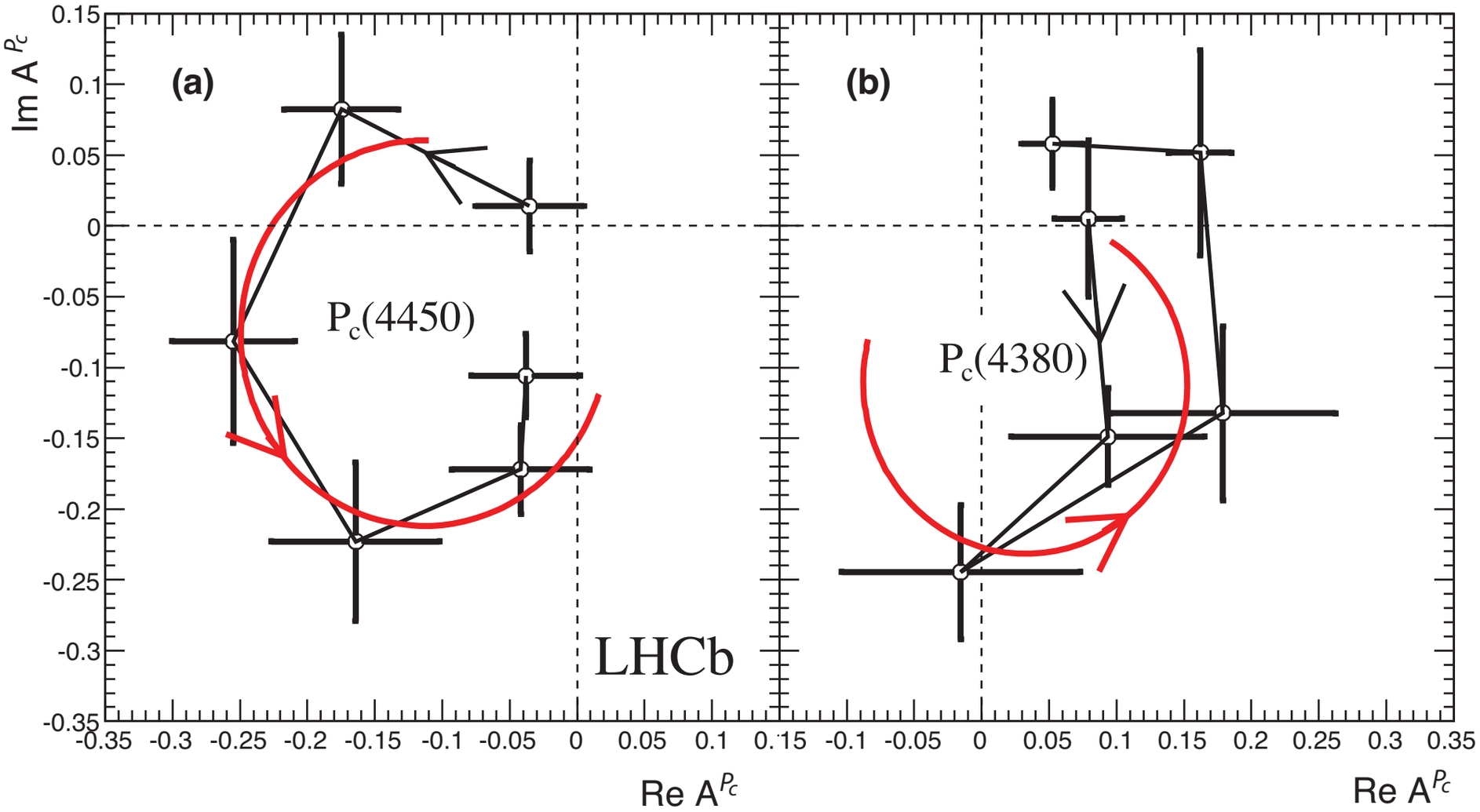

Figure 9: Fitted values of the real and imaginary parts of the amplitudes for the baseline ($3/2^-$, $5/2^+$) fit for a) the $P_c(4450)^+$ state and b) the $P_c(4380)^+$ state, each divided into six $m_{J/\psi p}$ bins of equal width between $-\Gamma_0$ and $+\Gamma_0$ shown in the Argand diagrams as connected points with error bars ($m_{J/\psi p}$ increases counterclockwise). The solid (red) curves are the predictions from the Breit-Wigner formula for the same mass ranges with M_0 (Γ_0) of 4450 (39) MeV and 4380 (205) MeV, respectively, with the phases and magnitudes at the resonance masses set to the average values between the two points around M_0. The phase convention sets $B_{0,\frac{1}{2}} = (1, 0)$ for $\Lambda(1520)$. Systematic uncertainties are not included.

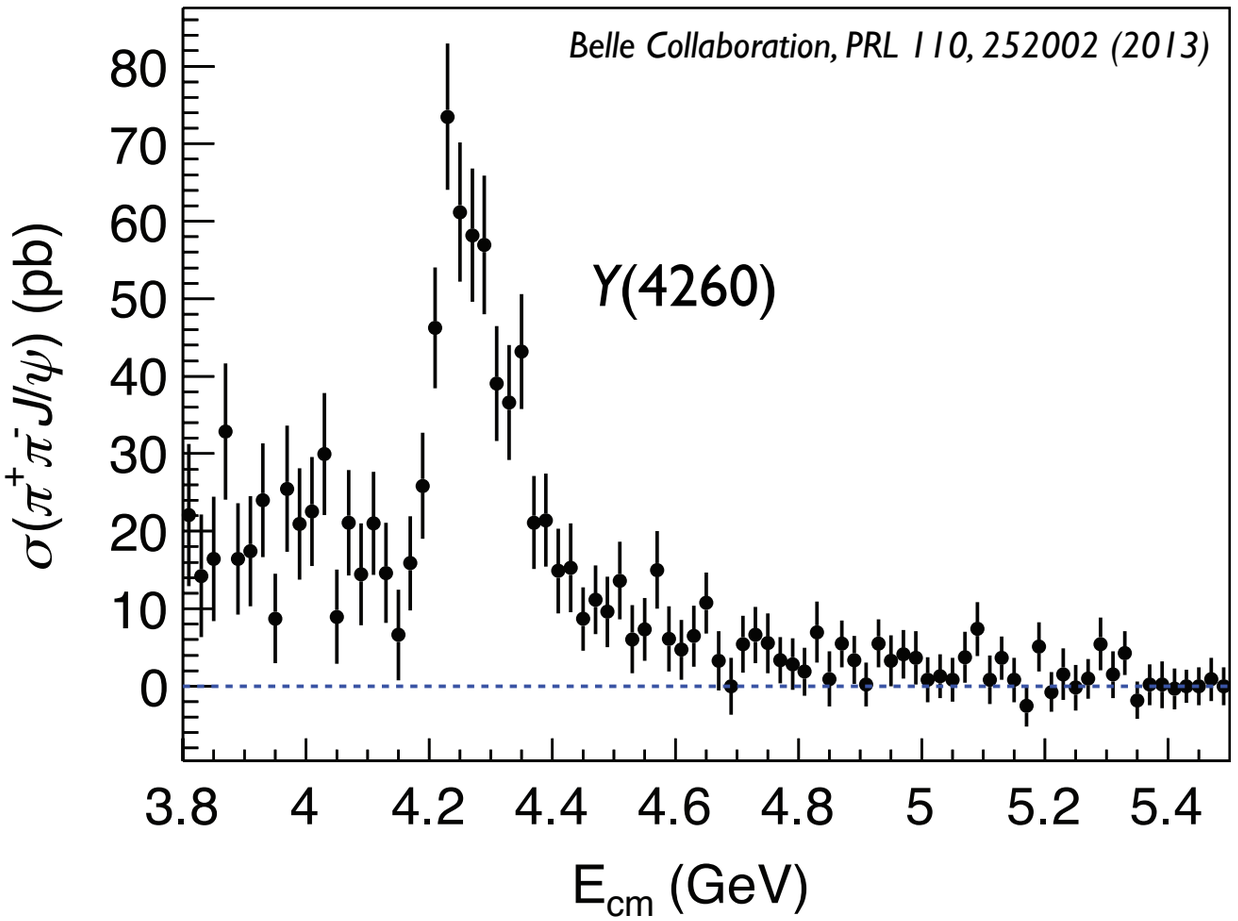
Belle Collaboration, PRL 110, 252002 (2013)
Y(4260)
$\sigma(\pi^+\pi^- J/\psi)$ (pb)
E_{cm} (GeV)

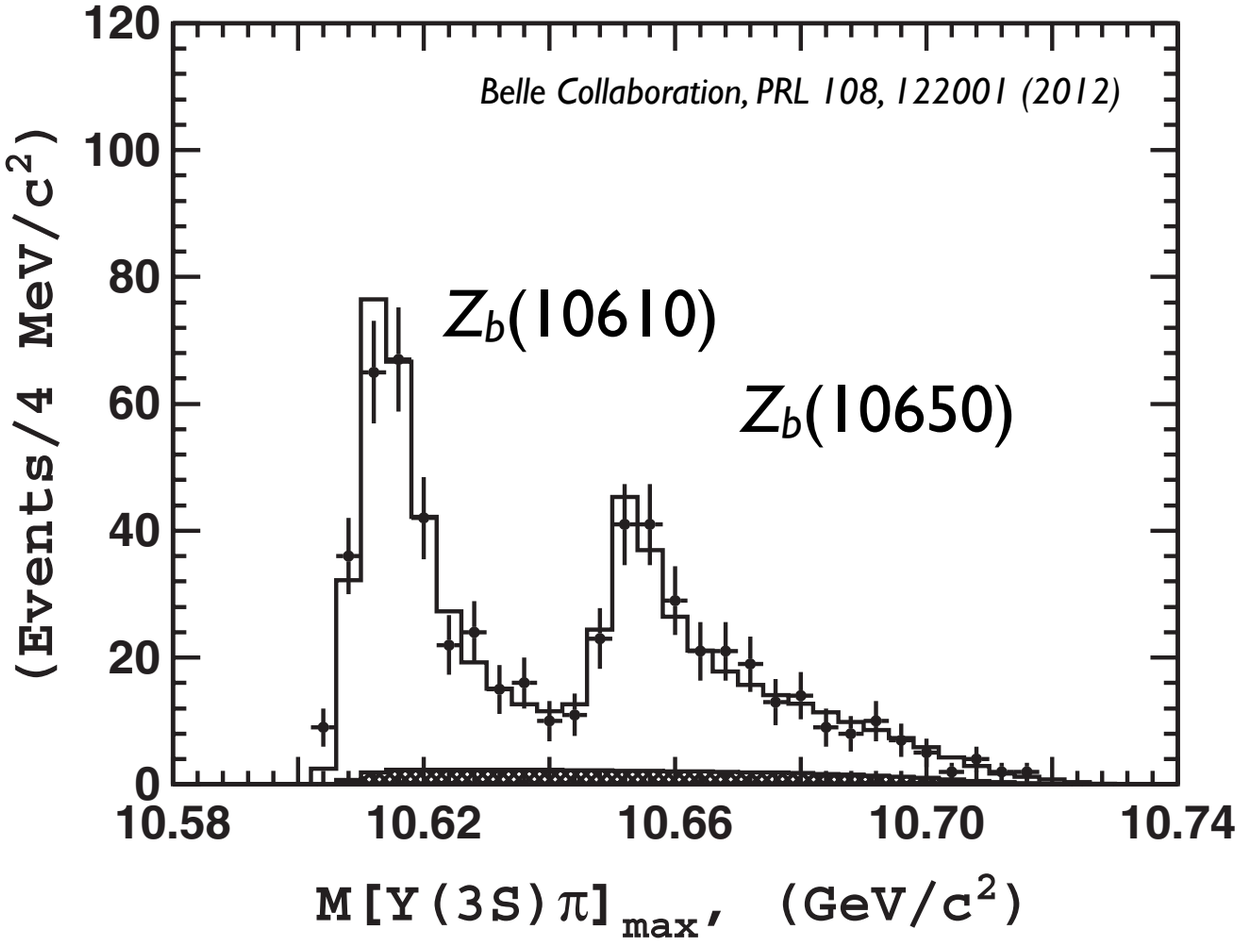
Belle Collaboration, PRL 108, 122001 (2012)
$Z_b(10610)$
$Z_b(10650)$
(Events/4 MeV/c^2)
$M[\Upsilon(3S)\pi]_{max}$, (GeV/c^2)

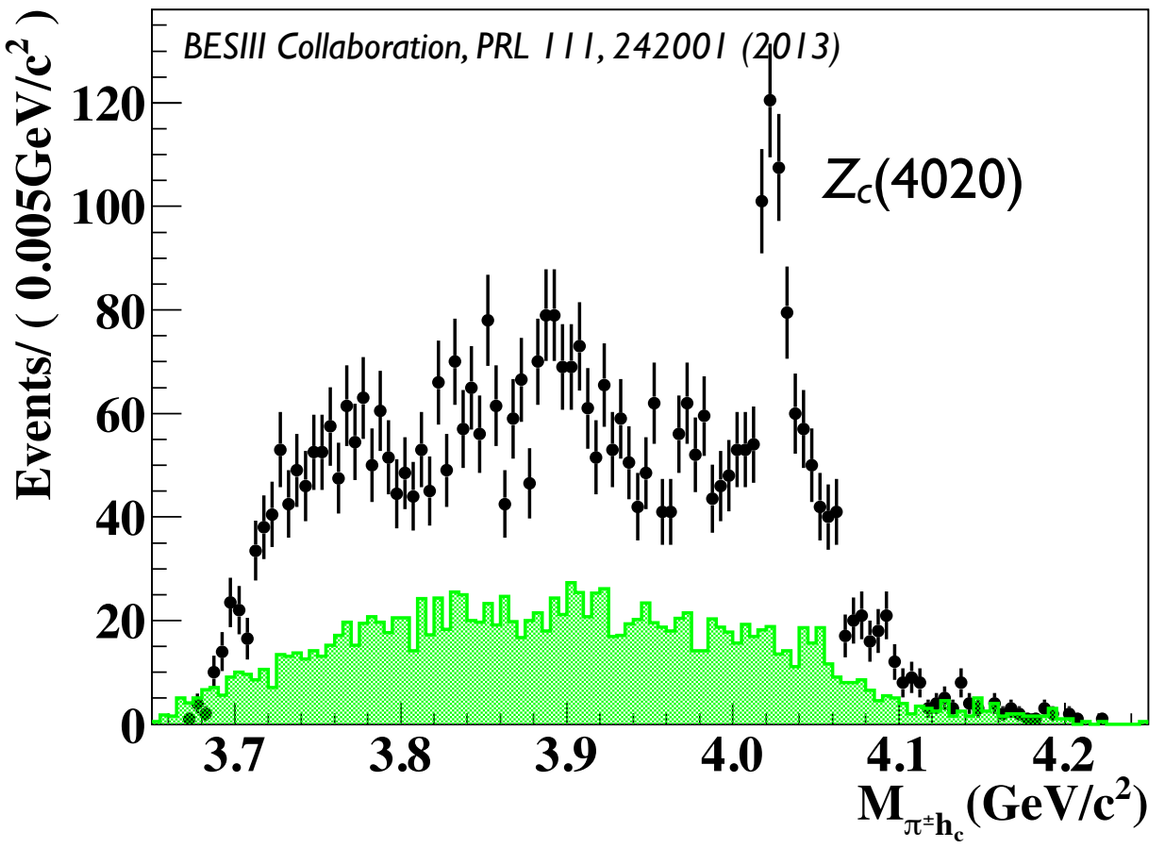
BESIII Collaboration, PRL 111, 242001 (2013)
$Z_c(4020)$
Events/ (0.005GeV/c^2)
$M_{\pi^\pm h_c}$(GeV/c^2)